Causality, Randomness, and the Microwave Background

Andreas Albrecht,[1] David Coulson,[2] Pedro Ferreira,[1,3] and Joao Magueijo[4]

[1]*Blackett Laboratory, Imperial College, Prince Consort Road, London SW7 2BZ, United Kingdom*
[2]*D. Rittenhouse Laboratory, University of Pennsylvania, Philadelphia, Pennsylvania 19104-6396*
[3]*Center for Particle Astrophysics, University of California, Berkeley, California 94720-7304*
[4]*Mullard Radio Astronomy Observatory, Cavendish Laboratory, Madingley Road, Cambridge CB3 0HE, United Kingdom and Department of Applied Mathematics and Theoretical Physics, University of Cambridge, Cambridge CB3 9EW, United Kingdom*

(Received 2 October 1995)

Fluctuations in the cosmic microwave background (CMB) temperature are being studied with ever increasing precision. Two competing types of theories might describe the origins of these fluctuations: "inflation" and "defects." Here we show how the differences between these two scenarios can give rise to striking signatures in the microwave fluctuations on small scales, assuming a standard recombination history. These should enable high resolution measurements of CMB anisotropies to distinguish between these two broad classes of theories, independent of the precise details of each.

PACS numbers: 98.70.Vc, 98.80.Cq

Modern experiments are producing a growing body of data on the fluctuations in the cosmic microwave background (CMB) [1]. The origin of these fluctuations may be due to defects [2,3] such as cosmic strings or textures, or an early period of cosmic inflation [4]. Our understanding of both pictures is sufficiently incomplete to allow a wide range of predictions from each [5,6]. Recent calculations of degree scale anisotropies from defects have focused on the case of a reionized thermal history [7]. Here, we consider a standard recombination universe, and show how fundamental differences between the defect and inflationary scenarios can leave sufficiently different signals as to allow the high resolution CMB measurements to distinguish between them.

The history of radiation can be separated into three epochs: At very early times (the "tight coupling" epoch) photons were tightly coupled to baryonic matter and together they behaved like a relativistic fluid in which pressure waves propagated at $c/\sqrt{3}$. As the universe expanded this coupling weakened, eventually producing today's "free-streaming" epoch where photon-matter interactions are negligible. These two epochs are linked by a "damping epoch" during which dissipation can diffuse perturbations [8–10]. We will focus our attention on the first of these epochs.

Because of their quantum nature, inflationary models predict an ensemble of possible states for the Universe, and the ensemble of subhorizon pressure waves of the photon-baryon fluid in an inflationary model are depicted in Fig. 1 (for fixed wavelength). Note that the ensemble is "phase focused," so that the entire ensemble achieves zero amplitude at the same instant in time [11]. These moments of zero amplitude occur at different times for different wave numbers, and the result is the striking oscillatory behavior in the power spectrum at the end of the tight-coupling epoch (Fig. 2 , solid curve).

In contrast, cosmic defects will drive subhorizon pressure waves in a random manner which tends to destroy the phase focusing (see Fig. 3). In many realistic cases (such as cosmic strings) we expect this effect to prevent an oscillatory power spectrum from emerging (Fig. 2, dashed curve). Figure 4 illustrates how these differences translate into observable features in the microwave sky. For other cases (such as cosmic texture) the phase decoherence of the evolving defect network is less effective, but

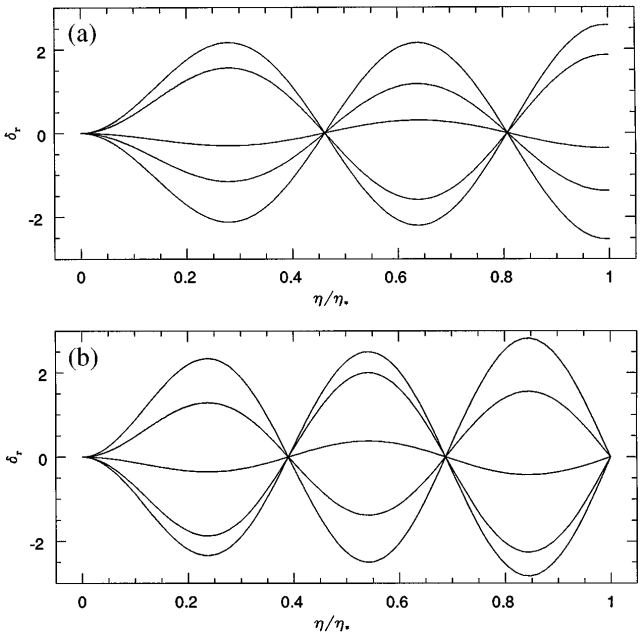

FIG. 1. Perturbations from inflation: Evolution of two different modes during the tight coupling era. While in (a) elements of the ensemble have nonzero values at $\eta_\star$, in (b), *all* members of the ensemble will go to zero at the final time ($\eta_\star$), due to the fixed phase of oscillation set by the "growing solution" initial conditions. The y axis is in arbitrary units.

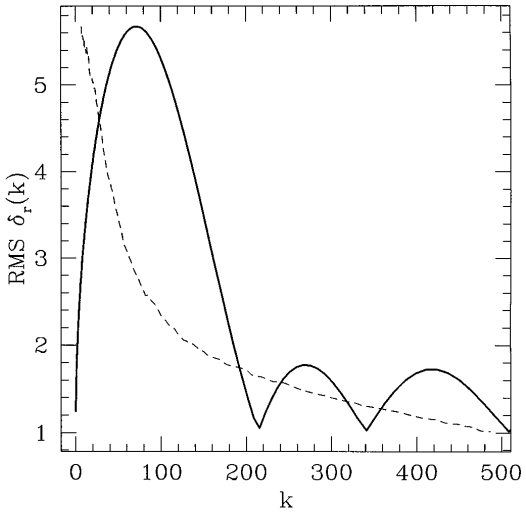

FIG. 2. The rms value of δ_r evaluated at decoupling ($\eta_\star$) for inflation (solid) and cosmic strings (dashed). For this figure we use $\mathcal{F}_{00} = [1 + 2(k\eta)^2]^{-1}$, $\mathcal{F}_D = 1/[1 + (2\pi/k\eta)^2]^2$, and $\eta_c = \eta/(1 + k\eta)$.

still the oscillations are of sufficiently different origin to leave a telltale signature [12,13].

We now treat each of these points in more technical detail. We evolve the radiation and matter fluids from some early epoch up to the time of last scattering and examine the processes which create or destroy the characteristic oscillations at decoupling. The calculation of the angular power spectrum (Fig. 4) involves additional physics and is treated in a companion Letter [13].

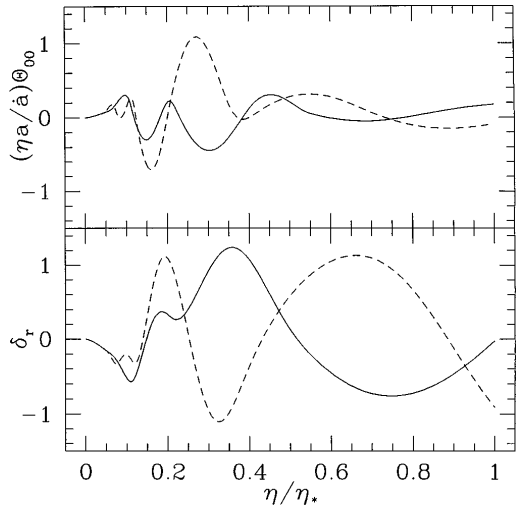

FIG. 3. Perturbations from defects: Evolution of $\delta_r(k)$ and the corresponding source Θ_{00} during the tight coupling era (Θ_D is not shown). Two members of the ensemble are shown, with matching line types. Because of the randomness of the source, the ensemble includes solutions with a wide range of values at $\eta_\star$. Unlike the inflationary case (Fig. 1) the phase of the temporal oscillations is not fixed. The y axis is in arbitrary units, and the source models are the same as for Fig. 2. The factor $\eta a/\dot{a}$ allows one to judge the relative importance (over time) of the Θ_{00} term in Eq. (2).

We work in the synchronous gauge, and use the variables of Ref. [14], extended to include a baryonic component. In Fourier space these are

$$\dot{\tau}_{00} = \Theta_D + \frac{1}{2\pi G}\left(\frac{\dot{a}}{a}\right)^2 \Omega_r \dot{s}[1 + R], \tag{1}$$

$$\dot{\delta}_c = 4\pi G \frac{a}{\dot{a}}(\tau_{00} - \Theta_{00}) - \frac{\dot{a}}{a}\left(\frac{3}{2}\Omega_c + 2[1 + R]\Omega_r\right)\delta_c - \frac{\dot{a}}{a}2[1 + R]\Omega_r s, \tag{2}$$

$$\ddot{s} = -\frac{\dot{R}}{1 + R}\dot{s} - c_s^2 k^2 (s + \delta_c). \tag{3}$$

Here $\tau_{\mu\nu}$ is the pseudo-stress-tensor $\Theta_D \equiv \partial_i \Theta_{0i}$, $\Theta_{\mu\nu}$ is the defect stress-energy, a is the cosmic scale factor, G is Newton's constant, δ_X is the density contrast, and Ω_X is the mean energy density over critical density of species X ($X = r$ for relativistic matter, c for cold matter, B for baryonic matter), $s \equiv \frac{3}{4}\delta_r - \delta_c$, $R = \frac{3}{4}\rho_B/\rho_r$, ρ_B and ρ_r are the mean densities in baryonic and relativistic matter, respectively, c_s is the speed of sound, and k is the comoving wave number. The dot denotes the conformal time derivative ∂_η.

The evolution described by these equations is very different for the two classes of theories we are considering.

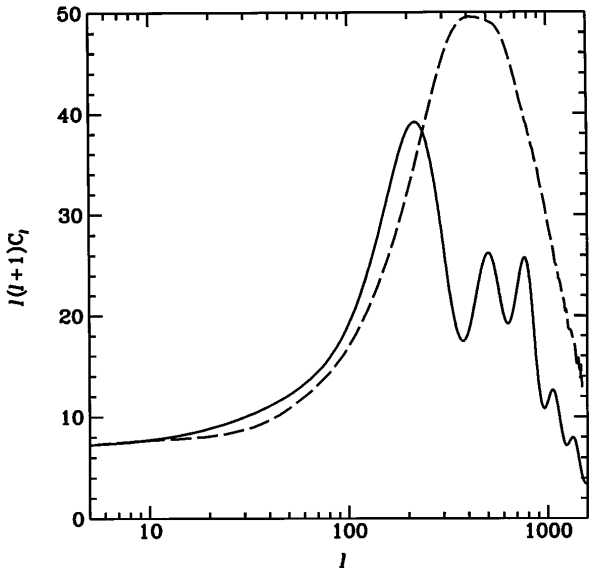

FIG. 4. Angular power spectrum of temperature fluctuations generated by cosmic strings (dashed) and arising from a typical model of scale invariant primordial fluctuations (solid) in arbitrary units. The all-sky temperature maps are decomposed into spherical harmonics $\frac{\Delta T}{T} = a_m^l Y_m^l$ from which one defines the angular power spectrum as $C_l = \frac{1}{2l+1}\sum_{-l}^{l} |a_m^l|^2$. The shape of the string curve for $l \lesssim 100$ (and thus the height of the peak) is very sensitive to existing uncertainties in string networks. We show only the scalar contribution, in arbitrary units. The string curve is from [13] where we use an extended Hu-Sugiyama formalism.

Consider first perturbations of a *primordial* origin, such as inflation, with no defects ($\Theta_{\mu\nu} = 0$). At reheating, all modes of interest are outside the horizon, with random phases and amplitudes chosen from some Gaussian distribution. On these superhorizon scales the radiation overdensity has one growing and one decaying solution (for example, in an inflationary model these behave as η^2 and η^{-2} in the radiation-dominated epoch). Just before horizon crossing these perturbations from inflation (and, more generally, most perturbations set by "initial conditions") will be dominated by the growing solution. If horizon crossing occurs in the tight-coupling epoch the growing solution will match onto a temporally oscillating solution, a pressure wave in the relativistic fluid.

The matching of a superhorizon pure growing mode to the subhorizon pressure wave forces the wave to have a unique temporal phase (for a given mode k) across the entire ensemble. For example, in Fig. 1(a) we see the evolution of several members of the ensemble for a specific k. For each realization (or member of the ensemble) the pressure wave has exactly the same phase. In Fig. 1(b) we pick another value of k for which, regardless of which element of the ensemble we take, all $\delta_r(k)$ lie on a node at $\eta_\star$, the end of the tight-coupling epoch. Figure 2 shows the resulting rms of $\delta_r(k, \eta_\star)$ (solid curve) for a range of k. The superhorizon growing condition gives $\delta_r(\eta_\star) = 0$ only for particular values of k, and the net result is the oscillatory spectrum above.

For cosmic defects the story is very different. In this case Eqs. (1)–(3) are sourced by the functions $\Theta_{00}(k, \eta)$ and $\Theta_D(k, \eta)$ (see, for example, [15]). Defects evolve in a highly nonlinear manner, and nothing short of a large, three-dimensional numerical simulation can be expected to give a $\Theta_{\mu\nu}(k, \eta)$ correct in every detail [14,16]. Here, we resort to a simplification which we expect to be a good approximation to the true defect evolution, and which certainly allows us to illustrate our main points.

We are interested in evaluating the radiation power spectrum at decoupling and therefore need not concern ourselves with detailed knowledge of the statistical properties of the defect network. It suffices to model correctly the one- and two-point correlation functions of the defect stress-energy. In Fourier space this means modeling the equal and *unequal* time correlation functions of Θ_{00} and Θ_D. (We will assume zero cross correlation between the two source functions, a freedom we can take without violating defect stress-energy conservation.) Let us construct functional forms for the equal time correlations first: Scaling of the network will restrict $\langle|\Theta_{00}(k, \eta)|^2\rangle = \frac{1}{\eta}\mathcal{F}_{00}(k\eta)$, where causality ensures that $\mathcal{F}_{00} \propto (k\eta)^0$ on large scales ($k\eta \ll 1$). The covariant conservation of the defect energy-momentum tensor forces $\langle|\Theta_D(k, \eta)|^2\rangle = (1/\eta^3)\mathcal{F}_D(k\eta)$, where $\mathcal{F}_D \propto (k\eta)^4$ on large scales. Depending on the type of defect, $\mathcal{F}_{00}$ and $\mathcal{F}_D$ will have different behavior on small scales; for cosmic strings, $\mathcal{F}_{00} \propto (k\eta)^{-2}$ on scales smaller than a fraction of the horizon [17], while for textures the turnover occurs on scales of order the horizon, and has a much steeper $(k\eta)^{-4}$ behavior [18]. (The caption to Fig. 2 gives one choice for these functions which models cosmic strings.)

Next, we note that the *un*equal time correlation functions [such as $\langle\Theta_{00}(k, \eta)\Theta_{00}(k, \eta + \Delta\eta)\rangle$] will go to zero at some finite value of $\Delta\eta$ characterized by a "coherence time" $\eta_c(k, \eta)$. The lack of long-time coherence is due to the fact that each mode is coupled in a highly nonlinear way to all the others. To a first approximation this coupling may be thought of as producing "random" kicks to a given mode, driving the unequal time correlation function to zero.

Using only the equal time correlation function and the coherence time we construct an ensemble of realizations of $\Theta_{00}(k, \eta)$ [and similarly $\Theta_D(k, \eta)$] in the following way: At the initial time η_i we choose a value for $\Theta_{00}(k, \eta_i)$ from a Gaussian distribution with variance given by $\langle|\Theta_{00}(k, \eta_i)|^2\rangle$. We next choose a time step from a distribution with mean value η_c, and choose a value for Θ_{00} at the new time, again from a distribution with variance given by this equal time correlation function at the new time. We continue this process until the final time is passed, and construct a smooth function using a cubic spline. The process is repeated many times to produce the ensemble of source histories.

All that remains is to choose initial conditions for the remaining variables of Eqs. (1)–(3), and here causality comes in. The formation of defects is assumed to occur against a completely homogeneous and isotropic background. It occurs in a finite time, and so is limited by causality to move matter only a finite distance (of order the horizon at the defect-producing phase transition). This translates into strong k^2 suppression of τ_{00} on large scales (see Refs. [14,19,20]). To reflect this we choose initial conditions with $\tau_{00}(\eta_i) = 0$ for all k. For a given initial defect source, $\tau_{00} = 0$ implies a "compensating" perturbation in the radiation and dark matter on large scales. The advantage of this formulation of the perturbation equations is that with such a choice of initial conditions, the compensating physical constraints are built-in and require no further attention.

Figure 3 shows the evolution of the δ_r in a cosmic string scenario, with the corresponding source evolution for each realization. The model is sufficiently incoherent to produce random phases in the pressure waves. Cosmic string networks are not well enough understood to dictate precisely the functions $\mathcal{F}_{D,00}$ and $\eta_c(\eta)$. We have explored a range of choices for these functions suggested by string simulations, and have found that they all have enough small scale power [and a small enough typical coherence time η_c (even the rather conservative choice $\eta_c = \eta$ does not give oscillations)] to be well inside the decoherence-dominated regime [21]. Thus in all these cases the power spectrum of the radiation at decoupling (the dashed curve in Fig. 2) does not show the oscillatory features found in the inflationary curve.

A particular high-coherence limit [taking $\Theta = (\langle|\Theta(k,\eta)|^2\rangle)^{1/2}$] has been explored by others in the context of the cosmic textures [12,18]. The models they used to calculate the microwave sky include none of the decohering effects we discuss here and, naturally enough, oscillations are produced. Crittenden and Turok [12] motivate the high-coherence limit by showing various correlation functions (including ones similar to Fig. 2) measured in large numerical simulations. The texture simulations show significant oscillations, indicating that a high level of coherence is present.

After the damping era, the CMB photons stream towards us and inhomogeneities in δ_r on different scales k will be converted into anisotropies $\Delta T/T$ seen today on different angular scales. Gravitational perturbations between the surface of last scattering and now will add on further anisotropies, but only on angular scales larger than the ones affected by the pre-$\eta_\star$ physics. Hence the $l > 100$ angular power spectrum will project into our sky the $\delta_r(k, \eta_\star)$ peak structure, the so-called "Doppler peaks" (softened somewhat by the effect of the radiation fluid's velocity). In [13] we account for all these effects by extending the formalism of Hu and Sugiyama [22] to include defects.

As an illustration, Fig. 4 gives the angular power spectrum of the brightness of the microwave sky for the standard CDM inflationary model and one of the string-based models considered in [13]. The string curve exhibits complete suppression of the secondary Doppler peaks, a signal which should be easily resolved by high resolution experiments (such as COBRAS/SAMBA [23]). Although the degree of secondary peak suppression can depend on the details of the defect model [13], we have found that realistic string models all appear to achieve complete suppression [21]. We emphasize that the shape of the string curve at low l and the peak position are still subject to uncertainty [13,21]. This is particularly true of the peak height, which is uncertain within an order of magnitude.

We have seen how the high degree of coherence which is present in inflationary scenarios (and some defect scenarios) leads to phase focusing of the subhorizon pressure waves. This effect leads to "secondary Doppler peaks" in the angular power spectrum. For defect scenarios the random effects of nonlinear defect evolution tend to decohere this focusing. Models representing cosmic strings exhibit a striking suppression of the secondary Doppler peaks in the angular power spectrum. Even in cases which are not so extreme, we expect that the decohering effects will lead to distinct observable signals in the angular power spectrum.

We thank R. Crittenden, M. Hindmarsh, J. Robinson, A. Stebbins, and N. Turok for interesting conversations. We thank N. Sugiyama for the use of the inflationary curve in Fig. 4. We acknowledge support from PPARC (A. A.) and DOE Grant No. DOE-EY-76-C-02-3071 (D. C). P. F. was supported by Programa Praxis XXI and the Center for Particle Astrophysics, a NSF Science and Technology Center at UC Berkeley, under Cooperative Agreement No. AST 9120005. J. M. thanks St. John's College, Cambridge, for support in the form of a research fellowship. A. A. and D. C. thank the Aspen Center for Physics, where some of this work was completed.

[1] M. White, D. Scott, and J. Silk, Annu. Rev. Astron. Astrophys. **32**, 319–370 (1994).
[2] T. W. B. Kibble, J. Phys. A **9**, 1387–1398 (1976).
[3] A. Vilenkin and P. Shellard, *Cosmic Strings and Other Topological Defects* (Cambridge University Press, Cambridge, 1994).
[4] P. Steinhardt, in Proceedings of the Snowmass Workshop on Particle Astrophysics and Cosmology, edited by E. Kolb and R. Peccei (Report No. astro-ph/9502024, 1995).
[5] R. Crittenden, J. R. Bond, R. L. Davis, G. P. Efstathiou, and P. J. Steinhardt, Phys. Rev. Lett **71**, 324–327 (1993).
[6] W. Hu, D. Scott, N. Sugiyama, and M. White (to be published); N. Sugiyama, Report No. astro-ph/9412025.
[7] D. Coulson, P. Ferreira, P. Graham, and N. Turok, Nature (London) **368**, 27–31 (1994).
[8] P. J. E. Peebles, *The Large Scale Structure of the Universe* (Princeton University Press, Princeton, NJ, 1980).
[9] A. Liddle and D. Lyth, Phys. Rep. **231**, 1–105 (1993).
[10] G. Efstathiou, in *Physics of the Early Universe*, edited by J. Peacock, A. Heaven, and A. Davis (IOP, Bristol, 1991), pp. 361–470.
[11] The spatial phase (giving the positions of zeros in space) is random, but the *temporal* phase is fixed; see, for example, A. Albrecht, P. Ferreira, M. Joyce, and T. Prokopec, Phys. Rev. D **50**, 4807–4820 (1994).
[12] R. Crittenden and N. Turok, Phys. Rev. Lett. **75**, 2642 (1995).
[13] J. Magueijo, A. Albrecht, D. Coulson, and P. Ferreira (to be published).
[14] U. Pen, D. N. Spergel, and N. Turok, Phys. Rev. D **49**, 692–729 (1994).
[15] J. C. R. Magueijo, Report No. MRAO/1782, DAMTP/94-101 (to be published).
[16] B. Allen, R. Caldwell, E. Shellard, A. Stebbins, and S. Veeraraghavan, in *The Proceedings of the Case Western Reserve University Workshop on CMB Anisotropies Two Years After COBE: Observations, Theory, and the Future, Cleveland, 1994*, edited by L. Krauss (World Scientific, Singapore, 1994), pp. 166–176.
[17] A. Albrecht and A. Stebbins, Phys. Rev. Lett. **68**, 2121–2124 (1992); **69**, 2615–2618 (1992).
[18] R. Durrer, A. Gangui, and M. Sakellariadou, Report No. astro-ph/9507035.
[19] S. Veeraraghavan and A. Stebbins, Astrophys. J. **365**, 37–65 (1990).
[20] J. Robinson and B. Wandelt, Phys. Rev. D **53**, 618 (1996).
[21] A. Albrecht, D. Coulson, P. Ferreira, and J. Magueijo (to be published).
[22] W. Hu and N. Sugyiama (to be published); W. Hu and N. Sugyiama, Phys. Rev. D **51**, 2599–2630 (1995).
[23] M. Tegmark and G. Efstathiou, Report No. MPI-PhT/95–62.